BIOCHEMISTRY
including biophysical chemistry & molecular biology

Article

pubs.acs.org/biochemistry

Kinetic Mechanism for the Flipping and Excision of 1,N^6-Ethenoadenine by AlkA

Erin L. Taylor and Patrick J. O'Brien*

Department of Biological Chemistry, University of Michigan, Ann Arbor, Michigan 48109, United States

Supporting Information

ABSTRACT: *Escherichia coli* 3-methyladenine DNA glycosylase II (AlkA), an adaptive response glycosylase with a broad substrate range, initiates base excision repair by flipping a lesion out of the DNA duplex and hydrolyzing the N-glycosidic bond. We used transient and steady state kinetics to determine the minimal mechanism for recognition and excision of 1,N^6-ethenoadenine (εA) by AlkA. The natural fluorescence of this endogenously produced lesion allowed us to directly monitor the nucleotide flipping step. We found that AlkA rapidly and reversibly binds and flips out εA prior to N-glycosidic bond hydrolysis, which is the rate-limiting step of the reaction. The binding affinity of AlkA for the εA-DNA lesion is only 40-fold tighter than for a nonspecific site and 20-fold weaker than for the abasic DNA site. The mechanism of AlkA-catalyzed excision of εA was compared to that of the human alkyladenine DNA glycosylase (AAG), an independently evolved glycosylase that recognizes many of the same substrates. AlkA and AAG both catalyze N-glycosidic bond hydrolysis to release εA, and their overall rates of reaction are within 2-fold of each other. Nevertheless, we find dramatic differences in the kinetics and thermodynamics for binding to εA-DNA. AlkA catalyzes nucleotide flipping an order of magnitude faster than AAG; however, the equilibrium for flipping is almost 3 orders of magnitude more favorable for AAG than for AlkA. These results illustrate how enzymes that perform the same chemistry can use different substrate recognition strategies to effectively repair DNA damage.

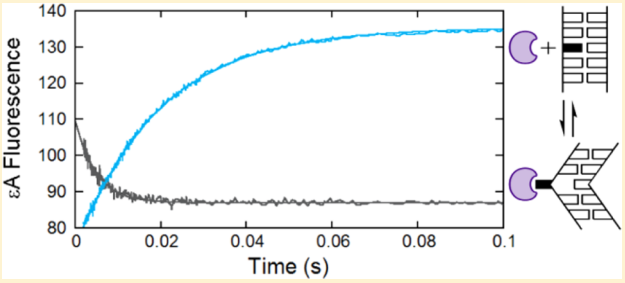

DNA nucleobases have multiple sites susceptible to alkylation damage, with alkylating agents coming from endogenous[1,2] and exogenous[3] sources such as methylmethanesulfonate (MMS) and methyl halides.[3,4] These lesions can exhibit cytotoxicity by blocking DNA replication (e.g., N^3-methyladenine, 3meA), cause mutations (e.g., 1-N^6-ethenoadenine, εA), or be relatively innocuous (e.g., N^7-methylguanine, 7meG).[4,5] Repair of cytotoxic and mutagenic lesions is vital for cell survival, and organisms have evolved many pathways to deal with DNA damage. In the case of small alkyl modifications, both direct reversal and base excision repair (BER) pathways are used. The BER pathway repairs damage caused by oxidation and deamination in addition to alkylation damage. This pathway is initiated by a variety of different DNA glycosylases that hydrolyze the N-glycosidic bond between the base lesion and sugar, generating an abasic site product. Subsequent enzymes nick the backbone, remove the residual deoxyribose phosphate, fill the gap, and seal the nick.[4,5] Two different superfamilies of glycosylases have evolved to recognize alkylative DNA damage. The first is the helix−hairpin−helix superfamily, exemplified by *Escherichia coli* 3-methyladenine DNA glycosylase II (AlkA), and the second is known as the alkyladenine DNA glycosylase (AAG) superfamily. Both AlkA and AAG exhibit a broad and overlapping substrate range.[5,6]

AlkA homologs are found mostly in prokaryotes and a few eukaryotes, whereas AAG homologs are found predominantly in plants and animals.[7,8] These two enzymes have been shown to have catalytic activity toward many of the same types of damaged bases, including methylated purines (e.g., 3meA and 7meG),[9,10] etheno adducts (e.g., εA),[11] and oxidatively damaged purines (e.g., hypoxanthine, hx).[12] Both enzymes also exhibit detectable activity toward undamaged bases.[13,14] While AAG and AlkA appear to be similar, they have distinct cellular roles in DNA repair. AlkA is upregulated as part of the adaptive (ada) response when *E. coli* is exposed to low levels of DNA alkylation. The overexpression of alkylation repair proteins allow *E. coli* to survive much higher levels of alkylating agents, which would have been toxic prior to adaptation.[15−17] In contrast, an adaptive response has not been observed in the regulation of AAG expression, and it appears to be constitutively expressed.

Previous studies of AAG and AlkA have led to similar proposed mechanisms for the recognition and excision of base lesions as summarized in Scheme 1. Given that damaged bases are rare, initial binding most often occurs at undamaged sites. After searching and locating a site of damage, both glycosylases gain access to the N-glycosidic bond by flipping the nucleotide 180° out of the DNA duplex. Crystal structures of AAG and AlkA demonstrate nucleotide flipping with the glycosylases

Received: October 31, 2014
Revised: December 19, 2014
Published: December 23, 2014

DOI: 10.1021/bi501356x
Biochemistry 2015, 54, 898−908

Scheme 1. Minimal Kinetic Mechanism for Base Excision by AlkA

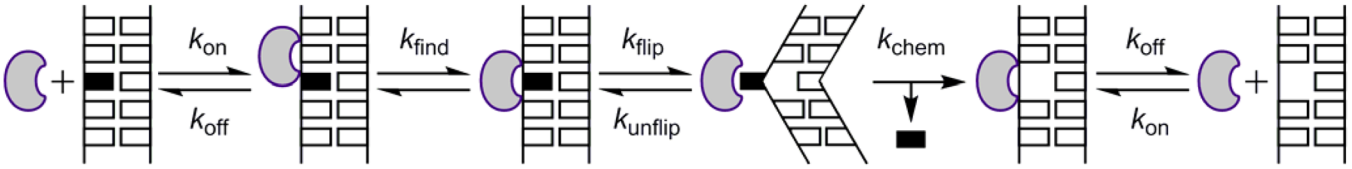

being bound to a flipped εA[18] and a flipped 1-azaribose sugar moiety,[19] respectively. Both enzymes use an active site carboxylate to position a water molecule for N-glycosidic bond hydrolysis (E125 in AAG[20] and D238 in AlkA[21,22]). For AAG-catalyzed excision of εA, the hydrolysis step (k_{chem}) is usually rate-limiting, but product release can be limiting for some substrates (e.g., hx).[23,24] For AlkA-catalyzed excision of hx, k_{chem} appears to be much slower than release of the abasic site.[25] It is likely that k_{chem} is also rate-limiting for AlkA-catalyzed excision of εA, but this model has not been tested. A complete kinetic and thermodynamic framework for the AAG-catalyzed reaction has been reported,[26] but much less is known about AlkA. Without direct observation of the binding and nucleotide flipping steps, it is not clear what step is rate-limiting for AlkA-catalyzed glycosylase activity.

In this study, the kinetic mechanism of AlkA-catalyzed base excision is determined for εA-DNA, a mutagenic adduct that is endogenously produced from reactions with lipid oxidation byproducts.[27−29] Although it has been established that both BER and direct repair play a role in the physiological repair of etheno adducts, their relative contributions differ in bacterial and mammalian cells. AAG-initiated BER and direct repair pathways appear to share responsibilities for repair of εA in the mouse.[30] In contrast, genetic experiments in *E. coli* suggest that both AlkA-initiated BER and direct repair are important for repair of etheno adducts,[31] but the direct repair pathway plays the predominant role for repair of εA.[32] However, AlkA exhibits similar catalytic efficiency for the excision of εA as for 3meA and other damaged and undamaged bases.[22] Therefore, we expect that the insights gained regarding the mechanism of εA excision will advance our understanding of AlkA and its broad substrate range. By taking advantage of the intrinsic fluorescence of εA, we can obtain a full kinetic and thermodynamic framework that can be directly compared to results of previous studies of AAG.[23]

We report the minimal kinetic and thermodynamic framework for AlkA-catalyzed flipping and excision of εA. We found that the steps leading up to the rate-limiting hydrolysis step are under rapid equilibrium. In particular, the εA flipping and unflipping steps are both very rapid, and the complex of AlkA with the flipped out εA is only marginally stable. In comparison, AAG forms a very stable complex with the flipped out εA.[23,26] This work provides a deeper understanding of how mechanistic differences affect the substrate recognition and catalytic efficiencies of two independently evolved DNA glycosylases and highlights the common features in the repair of damaged nucleotides.

MATERIALS AND METHODS

Preparation of Proteins. Full-length *E. coli* AlkA was expressed in BL21(DE3) *E. coli* cells.[21] Cultures were grown in LB to mid-log phase and induced with 0.1 mM IPTG for 4 h at 37 °C. Cells were lysed in lysis buffer [50 mM Tris-HCl (pH 8.6), 1 mM EDTA, 5% (v/v) glycerol, 50 mM β-ME, and 0.1 mg/mL PMSF] and centrifuged. The supernatant was passed through a DE52 column to remove DNA contamination and loaded onto an S-sepharose column. AlkA was eluted with a NaCl gradient (from 80 to 350 mM) and loaded onto a heparin-sepharose column, equilibrated with 50 mM Tris-HCl (pH 8.6), 10 mM NaCl, 1 mM EDTA, 10% (v/v) glycerol, and 10 mM β-ME. AlkA was eluted with a NaCl gradient (from 100 to 700 mM) and concentrated with an Amicon Ultra concentrator (10 kDa cutoff) to the desired concentration of ∼10 mg/mL. Aliquots were snap-frozen in liquid nitrogen and stored at −80 °C in 50 mM Tris-HCl (pH 8.6), 100 mM NaCl, 1 mM EDTA, 10 mM β-ME, and 10% (v/v) glycerol. Prior to being used, aliquots were thawed and diluted 1:1 in 1× reaction buffer without BSA (see Gel-Based General Glycosylase Activity Assay) and refrozen in liquid nitrogen for storage. For experiments, the diluted aliquots were thawed and stored at 4 °C for up to one month. UV absorbance was used to estimate the concentration of AlkA, and the active concentration was determined by titration with a tight binding inhibitor (see below).

Preparation of Oligonucleotides. For this study, 19- and 25-mer oligonucleotides were used (Figure 1), the 19-mers having an asymmetrically placed lesion.[25] Oligonucleotides were not labeled unless noted in this section, in which case a 5′ 6-fluorescein (FAM) or a 6-hexachlorofluorescein (HEX) label was present on the lesion-containing strand. Desalted DNA substrates were purchased from Integrated DNA Technologies (IDT) or the Keck Center at Yale University (New Haven, CT). Oligonucleotides were purified via denaturing polyacrylamide gel electrophoresis (PAGE), extracted, and desalted by reverse phase C18 columns (Sep-Pak, Waters). The concentration was determined from the A_{260} and the calculated extinction coefficient. For εA substrates, 9400 M^{-1} cm^{-1} was subtracted from the extinction coefficient of an undamaged substrate (adenine in place of εA) to account for the weaker absorbance of εA. The extinction coefficient of pyrrolidine substrates was calculated by replacing the pyrrolidine with dSpacer.

Abasic DNA was produced by incubating 25ThxC DNA with excess Δ80 AAG[20] at 37 °C for at least 50 turnovers. The DNA

```
19TxC:          5′-CAT CCT x CCT TCT CTC CAT-3′
                3′-GTA GGA T GGA AGA GAG GTA-5′

19AxA:          5′-CAT CAA x AAT TCT CTC CAT-3′
                3′-GTA GTT T TTA AGA GAG GTA-5′

25TxC: 5′-CGA TAG CAT CCT x CCT TCT CTC CAT-3′
       3′-GCT ATC GTA GGA T GGA AGA GAG GTA-5′
```

Figure 1. Oligonucleotide substrates used in this study. The nomenclature #NxN describes the length, flanking bases, and lesion [x being ε = εA, hx = hypoxanthine, py = pyrrolidine, A = adenine (undamaged), and ab = abasic]. x-DNA denotes the full nucleotide, while x describes the nucleobase.

DOI: 10.1021/bi501356x
Biochemistry 2015, 54, 898−908

was extracted via phenol and chloroform and desalted with an Illustra MicroSpin G-25 column (GE Healthcare) that had been equilibrated with annealing buffer [10 mM NaMES (pH 6.5) and 50 mM NaCl]. The concentration of the DNA was determined by the absorbance of the FAM label and corrected for purity as determined by denaturing PAGE (>95% pure).

Oligonucleotides were annealed with a 1.2-fold excess of the complementary strand by being heated to 95 °C for 3 min and cooled to 4 °C at a rate of 0.2 °C/s. Previous work shows that the excess complementary strand does not affect the observed rate constants.[25]

Gel-Based General Glycosylase Activity Assay. Unless otherwise noted, all discontinuous glycosylase activity assays were performed by incubating AlkA and a DNA substrate at 37 °C in reaction buffer [50 mM NaMES (pH 6.1), 100 mM ionic strength (controlled with NaCl), 1 mM EDTA, 1 mM DTT, and 0.1 mg/mL BSA]. If glycerol was present, a concentration of 10% (v/v) was used. At varying time points, the aliquots of the reaction mixture were quenched in 0.2 M NaOH and placed on ice to prevent the base-catalyzed ring opening of εA. The samples were then heated for 12 min at 70 °C, and varying volumes of loading buffer (98% formamide, 1 mM EDTA, bromophenol blue, and xylene cyanol) were added to ensure 5−200 fmol of DNA was analyzed by denaturing PAGE [20% (w/v) acrylamide, 1× TBE, and 6.6 M urea]. Gels were imaged using a Typhoon Trio Fluorescence imager (GE Healthcare) with a 488 nm excitation and a 520 nm band-pass filter to detect fluorescein. The fraction of product for each time point was calculated by dividing the intensity of the product band by the sum of intensities of both product and substrate bands in each lane.

Determination of the Concentration of Active AlkA. A tight binding inhibitor (pyrrolidine-containing DNA) was used to titrate the amount of active AlkA.[25,33] AlkA (100 or 200 nM) was incubated with excess 5′FAM-19ThxC substrate (500 nM) and varying concentrations of 5′HEX-25TpyC inhibitor (0−800 nM) under the glycosylase assay conditions described above. 19ThxC was used in place of 19TεC as AlkA binds hypoxanthine with a weaker affinity (data not shown), making the pyrrolidine DNA a better inhibitor. The fraction product versus time was fit by linear regression as described in Multiple-Turnover Glycosylase Activity. The relative activity was calculated by normalizing to the reaction rate without inhibitor. The concentration of active AlkA was determined by using the quadratic binding equation (eq 1)

$$\frac{V_{obs}}{V_{max}} = 1 - \frac{K_d + [E] + [I] - \sqrt{(K_d + [E] + [I])^2 - 4[E][I]}}{2[E]} \quad (1)$$

where K_d is the dissociation constant for py binding and E and I represent AlkA and the py inhibitor, respectively. AlkA was found to be 85% active compared to the estimation that was based on the UV absorbance (Figure S1 of the Supporting Information). The active concentration was used for all subsequent experiments.

Multiple-Turnover Glycosylase Activity. Excess 5′FAM-19TεC DNA (10−200 nM) was incubated with 1 nM AlkA under the glycosylase assay conditions. The first 8% of reactions (5% for 19ThxC reactions) were used to obtain the rate of reaction (V_{obs}), ensuring linearity as product inhibition occurs after these limits (data not shown).[25] Values of $V_{obs}/[E]$ were plotted versus DNA concentration and fit by the Michaelis−Menten equation (eq 2)

$$\frac{V_{obs}}{[E]} = \frac{k_{cat}[S]}{K_m + [S]} \quad (2)$$

where k_{cat} is the maximal turnover rate constant, S is the substrate, E is AlkA, and K_m is the concentration at which the observed rate constant is half the maximal rate constant.

Single-Turnover Glycosylase Activity. Excess AlkA (at least 2-fold) was incubated with 5′FAM-19TεC DNA for single-turnover reactions under the glycosylase assay conditions. The DNA concentration ranged from 5 to 50 nM, and the AlkA concentration ranged from 10 nM to 5 μM. In some cases, reactions were compared with the same concentration of AlkA and two different concentrations of DNA to ensure that single-turnover conditions were met. The fraction product was fit by a single exponential (eq 3)

$$F = A[1 - \exp(-k_{obs}t)] + c \quad (3)$$

where F is the fraction product, A is the amplitude, k_{obs} is the observed single-turnover rate constant, t is the reaction time, and c is the amount of preexisting abasic DNA.

The concentration dependence of the single-turnover rate constant was fit by a hyperbolic dependence (eq 4)

$$k_{obs} = \frac{k_{max}[E]}{K_{1/2} + [E]} \quad (4)$$

where k_{max} is the maximal single-turnover rate constant, E is AlkA, and the $K_{1/2}$ is the concentration of AlkA at which k_{obs} is 50% of the k_{max} value.

Equilibrium Inhibition by Undamaged DNA and the Abasic DNA Product. AlkA (5 nM) was incubated under normal glycosylase assay conditions with excess DNA. Ratios of inhibitor (25TAC or 5′FAM-25TabC) to substrate (5′FAM-19TεC) were varied, while the total DNA concentration was kept constant (1 μM for undamaged DNA reactions or 500 nM for abasic DNA reactions). Linear fits to the fraction product data were performed as described in Multiple-Turnover Glycosylase Activity, and the observed rate was normalized to the reaction rate without inhibitor. A competitive inhibition model (eq 5) was used to fit the [I]/[S] dependence, yielding the ratio of the K_m for substrate to the K_i for inhibitor (K_d for abasic DNA binding).[24] For the undamaged DNA, a microscopic K_d value was determined by multiplying the K_i value by the number (N) of nonspecific binding sites on the 25TAC inhibitor. N was calculated with eq 6, in which L is the total length of the oligo, l is the site size or footprint of the enzyme (8 bp),[19] and the number of sites is doubled to account for both DNA strands. This calculation assumes that AlkA would bind with equal affinity to all nonspecific sites. For the 25TAC inhibitor, the number of binding sites was calculated to be 36 [2 × (25 − 8 + 1) = 36].

$$\frac{V_{obs}}{V_{max}} = \frac{1}{\frac{[I]}{[S]} \times \frac{K_m}{K_i} + 1} \quad (5)$$

$$N = 2(L - l + 1) \quad (6)$$

εA Quenching by AlkA under Steady State Conditions. To measure the stoichiometry of binding of AlkA to εA, the εA fluorescence of 400 nM 19AεA DNA was monitored

DOI: 10.1021/bi501356x
Biochemistry 2015, 54, 898−908

with varying concentrations of AlkA. A PTI QuantaMaster fluorometer using FeliX software was used to measure the εA fluorescence (excitation of 316 nm and emission of 408 nm; both 6 nm band-pass). Reactions were performed at 25 °C in a HEPES, pH 7.5 reaction buffer [50 mM HEPES, 100 mM ionic strength (controlled with NaCl), 1 mM EDTA, and 1 mM DTT] to slow excision of εA. The spectra were recorded within 1 min of AlkA and DNA mixing. The quenching of the εA was normalized to the fluorescence of free 19AεA and fit to a 1:1 binding equation (eq 7)

$$F = 1 - \frac{A\left[K_d + [E] + [S] - \sqrt{(K_d + [E] + [S])^2 - 4[E][S]}\right]}{2[S]} \quad (7)$$

where F is the normalized fluorescence, A is the amplitude of the fluorescence change, E and S are AlkA and the substrate, respectively, and the K_d is the dissociation constant of εA binding.

Stopped-Flow Kinetics. Pre-steady state kinetics experiments were performed on a Hi-Tech SF-61DX2 Stopped-Flow System using Kinetic Studio (TgK Scientific). The fluorescence of εA was observed using an excitation wavelength of 313 nm and a WG360 long-pass emission filter. Excess AlkA and 100 nM (final concentration) 19AεA or 19TεC DNA (in glycosylase assay buffer with no BSA) were mixed at 25 °C. The εA fluorescence was measured for 2 s, with the average of three independent measurements fit by a single exponential (eq 3). The AlkA concentration dependence was fit with a hyperbolic function (eq 4). The k_{max} is independent of AlkA concentration and describes the nucleotide flipping step, which is an approach to equilibrium (eq 8). The value of k_{on} was estimated by assuming that at a saturating AlkA concentration (850 nM), the $k_{on,obs}$ is at least 10-fold faster than the $k_{flip,obs}$ (eq 9).

$$k_{max} = k_{flip,obs} = k_{flip} + k_{unflip} \quad (8)$$

$$k_{on,obs} = k_{on}[AlkA] \geq 10k_{flip,obs} \quad (9)$$

To measure the rate of dissociation from undamaged DNA, 5 μM 19AεA substrate was mixed with a preformed complex of 1 μM AlkA and 500 nM 25TAC. A single phase was observed up to 0.05 s and fit by a single exponential. The k_{off} value was calculated using eq 10

$$\frac{1}{k_{obs}} = \frac{1}{k_{flip,obs}} + \frac{1}{k_{off}} \quad (10)$$

where k_{obs} is the rate constant for dissociation of AlkA from undamaged DNA and subsequent binding to εA-DNA and $k_{flip,obs}$ is the rate constant of the association of free AlkA with the same εA-DNA.

Pulse-Chase Glycosylase Assays. Single-turnover assays were performed with 1 μM AlkA and 100 nM 5′FAM-19TεC substrate and fit by a single exponential as described for Single-Turnover Glycosylase Activity. Pulse-chase reaction mixtures were aged for 20 s prior to the addition of 10 μM 25TpyC chase, and reactions were fit by a straight line with a slope of zero. Reactions with substrate and chase premixed before addition of AlkA and a no enzyme control were also performed, showing no εA cleavage. The observed rate constant for dissociation ($k_{off,obs}$) is given by eq 11

$$k_{off,obs} = \frac{k_{max}}{A} - k_{max} \quad (11)$$

where A is the amplitude in the pulse-chase reaction and k_{max} is the maximal rate from the single-turnover reaction.

Double-Mixing Stopped-Flow Kinetics. Stopped-flow experiments were performed as described above with the following changes. The AlkA and DNA were mixed and aged for 1 or 5 s and then mixed with chase. The final concentrations after mixing were 425 nM AlkA, 200 nM 19AεA DNA, and 3 or 10 μM 25TpyC chase. The εA fluorescence was measured for 2 s, with averages of three measurements fit by a single exponential (eq 3) giving a $k_{off,obs}$ value, defined in eq 12. The k_{unflip} value was calculated according to eq 13 (rearranged from eqs 8 and 12).

$$k_{off,obs} = k_{unflip}\left(\frac{k_{off}}{k_{off} + k_{flip}}\right) \quad (12)$$

$$k_{unflip} = \frac{k_{off,obs}k_{off} + k_{off,obs}k_{flip,obs}}{k_{off,obs} + k_{off}} \quad (13)$$

RESULTS

AlkA-Catalyzed Excision of εA. To determine the kinetic framework for AlkA-catalyzed εA excision, both multiple- and single-turnover kinetics were measured using a gel-based discontinuous assay. Whereas the multiple-turnover rate monitors the entire reaction, including product release, the single-turnover reaction monitors only steps up to and including N-glycosidic bond hydrolysis, which is irreversible under these conditions (Scheme 1).

Most previous studies of AlkA have included glycerol as a buffer component, but we excluded it because AlkA catalyzes a side reaction with abasic sites to form a glycerol adduct.[34] Single-turnover glycosylase assays in the presence and absence of 10% glycerol showed that AlkA is well-behaved and slightly more active in the absence of glycerol (Figure S2 of the Supporting Information). We used an asymmetric 19-mer oligonucleotide containing a single site of damage [19TεC (Figure 1)], because the binding of multiple AlkA molecules can be inhibitory when the lesion site is located different distances from a DNA end.[25] This inhibitory behavior was previously observed for the excision of hypoxanthine (hx) from a 25-mer DNA in buffers containing glycerol, and we confirmed that similar behavior is observed for the excision of εA from a 25-mer DNA in the absence of glycerol (Figure S3 of the Supporting Information). Therefore, the 19TεC substrate was employed for the glycosylase kinetic assays that are described below.

Multiple-turnover kinetics were first determined by incubating AlkA with excess DNA substrate. The initial rates of reaction were calculated by fitting the first 8% of reaction by a straight line (Figure 2A), because inhibition by the abasic product can be detected above that percentage (data not shown).[25] The dependence on the concentration of εA-DNA followed Michaelis−Menten behavior with a k_{cat} value of 0.24 ± 0.06 min^{-1} and a K_m value of 15 ± 13 nM (Figure 2B). In experiments with a greater concentration of AlkA, there was no evidence of a burst phase (data not shown). This is similar to what was previously observed with hx-DNA[25] and suggests that the rate-limiting step is N-glycosidic bond hydrolysis or a preceding step.

DOI: 10.1021/bi501356x
Biochemistry 2015, 54, 898−908

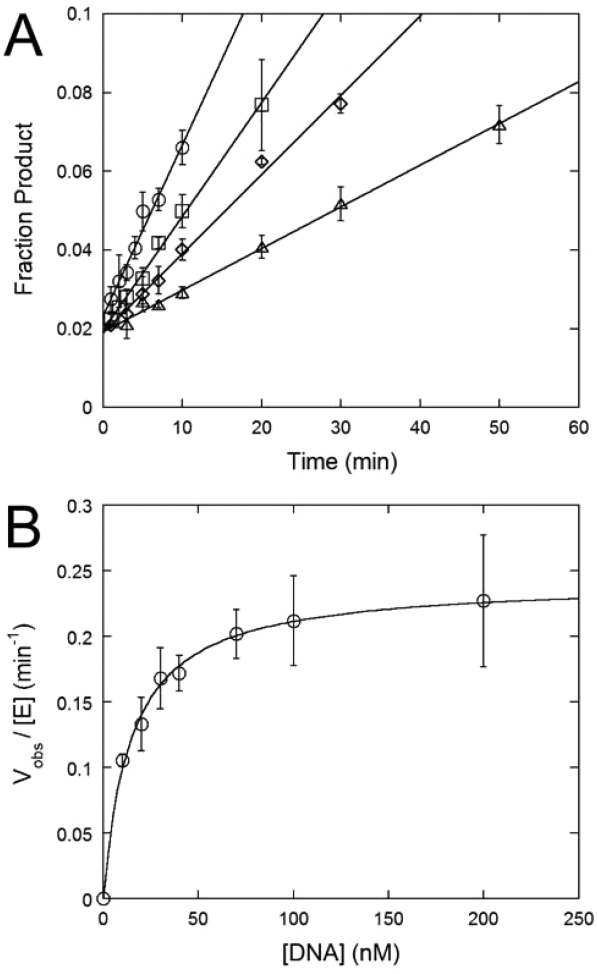

Figure 2. Multiple-turnover excision of εA by AlkA. (A) Representative time course for excision of 19TεC substrate [40 (○), 70 (□), 100 (◇), and 200 nM (△)] by AlkA (1 nM). Linear fits were performed for the first 8% of the reaction to ensure linearity and avoid product inhibition. The average of duplicate reactions is shown ± the standard deviation (SD). (B) The substrate concentration dependence follows Michaelis–Menten kinetics with a k_{cat} value of 0.24 ± 0.06 min^{-1} and a K_m value of 15 ± 13 nM. The average ± SD is shown (n = 4). This K_m value is poorly defined, but the sensitivity of the assay precludes measurement of steady state kinetics at lower DNA concentrations. Note that a wider concentration range is possible for single-turnover kinetics (Figure 3B).

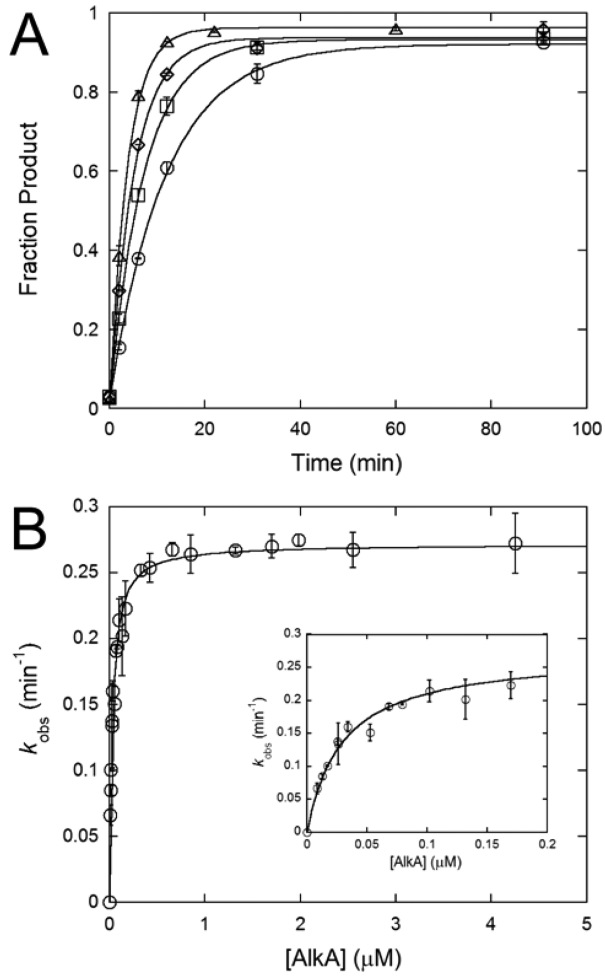

Figure 3. Single-turnover excision of εA by AlkA. (A) Representative time course for single-turnover excision of 19TεC substrate (5 or 50 nM) by varying concentrations of AlkA [12.75 nM (○), 25.5 nM (□), 68 nM (◇), and 2.55 μM (△)]. The data were fit by a single exponential. The average of duplicate reactions is shown ± SD. (B) Hyperbolic dependence of the single-turnover rate constant on the AlkA concentration with a k_{max} of 0.27 ± 0.01 min^{-1} and a $K_{1/2}$ value of 29 ± 3 nM. The inset shows an expanded plot of the lowest AlkA concentrations. The average of duplicate reactions is shown ± SD.

We next measured the single-turnover glycosylase reaction with AlkA in excess over the 19TεC substrate. In all cases, the reaction progress curve followed a single exponential (Figure 3A), and the values of the observed single-turnover rate constant (k_{obs}) were obtained for each enzyme concentration. The AlkA concentration dependence was fit by a hyperbolic dependence (Figure 3B), with a maximal single-turnover rate constant (k_{max}) of 0.27 ± 0.01 min^{-1} (0.0045 s^{-1}) and a $K_{1/2}$ value of 29 ± 3 nM. These kinetic parameters are almost identical to those observed in the multiple-turnover experiments, suggesting that the same step is rate-limiting for single-turnover and multiple-turnover conditions. Although these data are consistent with either rate-limiting conformational change, such as nucleotide flipping or rate-limiting N-glycosidic bond hydrolysis, direct measurement of nucleotide flipping supports the latter model (see below).

Affinity of AlkA for Abasic Product and Undamaged DNA. To measure the affinity of AlkA for binding to the abasic product and undamaged DNA, we performed multiple-turnover experiments with mixtures of the 19TεC substrate and 25-mer DNA competitors that either contained a single abasic site or were undamaged. With a constant amount of total DNA, the competitive inhibition can be monitored as previously described.[24] The relative activity is plotted as a function of the ratio of inhibitor to substrate, and the curve fit provides the relative K_m/K_i values (Figure 4). The K_i values were calculated using the independently determined K_m for εA-DNA (Figure 2B). For the abasic-containing DNA, this K_i value of 1.2 ± 0.1 nM is equal to the dissociation constant (K_d). This tight binding to the abasic site corroborates the significant product inhibition that occurs under multiple-turnover conditions. For the undamaged DNA, the observed inhibition constant is 33 ± 16 nM, which reflects the affinity of AlkA for the total number of nonspecific binding sites along the 25-mer undamaged DNA duplex. Assuming a site size of 8 bp,[19] there are 36 overlapping binding sites (N) on the undamaged DNA (eq 6) with an

DOI: 10.1021/bi501356x
Biochemistry 2015, 54, 898–908

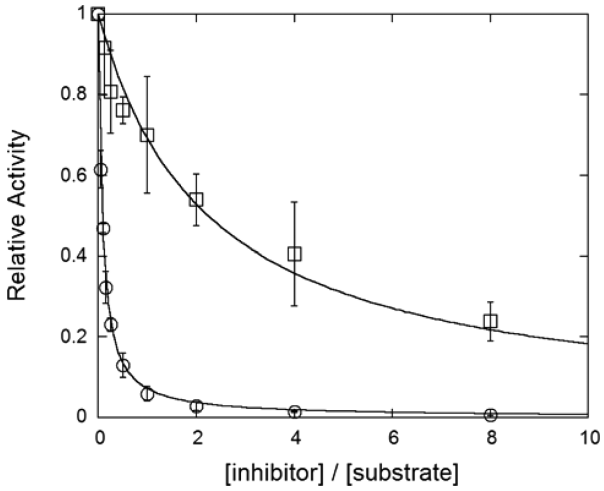

Figure 4. Affinity of AlkA for abasic and undamaged DNA determined with competition experiments. Multiple-turnover competition between the 19TεC substrate and 25TabC (○) or 25TAC (□) inhibitor DNA. The initial rate of product formation (up to 8%) was measured, and the relative activity (V_{obs}/V_{max}) was fit by the model for competitive inhibition (eq 5). The average ± SD is shown ($n \geq 3$). The K_m/K_i values for abasic and undamaged inhibitor were 12.8 ± 0.8 and 0.45 ± 0.15, respectively. Using the K_m value of 15 nM for εA-DNA (Figure 2B), $K_{i,obs}$ values of 1.2 ± 0.1 nM for the abasic product and 33 ± 16 nM for undamaged DNA were calculated. This macroscopic value for undamaged DNA can be used to calculate a microscopic $K_{d,nsDNA}$ value of 1.2 μM for an individual nonspecific site (see Materials and Methods).

average K_d value of 1.2 μM for an individual nonspecific binding site ($K_{d,nsDNA} = NK_i = 36 \times 33$ nM = 1.2 μM). Additional experiments with different DNA duplexes gave the same dissociation constant for an average nonspecific site (Figure S4 of the Supporting Information; $K_{d,nsDNA}$ = 1.2 ± 0.2 μM).

Before proceeding to stopped-flow experiments, we repeated some of the glycosylase assays at a lower temperature because we expected that DNA binding and nucleotide flipping might be very fast and would be more easily measured at 25 °C. The rate of the N-glycosidic bond cleavage step, measured with saturating AlkA, was found to be ∼3-fold slower at 25 °C [0.080 ± 0.003 min^{-1} = 0.0013 s^{-1} (Figure S5 of the Supporting Information)]. The steady state kinetic parameters and the competition with undamaged DNA were also investigated at 25 °C, and very similar K_m and K_d values were obtained (Figure S6 of the Supporting Information). These observations suggest that the main difference between AlkA activity at 25 and 37 °C is that the rate-limiting step (N-glycosidic bond cleavage) is slower at the lower temperature.

DNA Binding and Nucleotide Flipping by AlkA. We sought to use the intrinsic fluorescence of εA to monitor the DNA binding and nucleotide flipping steps conducted by AlkA. The difference in fluorescence between free DNA and bound DNA provides the signal for detecting binding and nucleotide flipping. Our efforts were guided by previous studies of the binding of AAG to εA-DNA.[23] It is advantageous to use different sequence contexts in which the basal εA-DNA fluorescence is either high or low, because it is difficult to predict how strongly the fluorescence will be quenched upon binding to the protein. As the fluorescence of 19TεC is relatively low in duplex DNA, we also prepared a 19AεA substrate that has much higher basal fluorescence (Figure 1).[23]

To establish if AlkA binding causes a detectable change in εA-DNA fluorescence, we performed steady state fluorescence experiments by incubating different concentrations of AlkA with the 19AεA DNA. Enzyme and substrate were incubated for 1 min to give time for binding to occur, but prior to N-glycosidic bond cleavage. The fluorescence of the εA-DNA was strongly quenched by 1 equiv of AlkA (Figure 5A), suggesting that a monomer of AlkA tightly binds to each εA lesion site. It is likely that the decrease in εA-DNA fluorescence is attributed to interaction between the flipped out εA base and the tryptophan residues that line the AlkA active site.[19]

We next used stopped-flow fluorescence to monitor the kinetics of DNA binding and nucleotide flipping. When the 19AεA substrate was rapidly mixed with excess AlkA, a fast quenching of εA fluorescence was detected that followed a single exponential (Figure 5B) and exhibited a good signal-to-noise ratio (Figure 5C). The rate constants calculated for each AlkA concentration were roughly fit by a hyperbolic function, but the observed rate constant was almost fully saturated even at the lowest concentration of AlkA (Figure 5D). The concentration independence at a high concentration of AlkA suggests that the εA quenching step being observed corresponds to the nucleotide flipping step ($k_{flip,obs}$ = 242 ± 11 s^{-1}), as a DNA binding event would be dependent on AlkA concentration. The observed rate constant for formation of the flipped out complex is equal to the sum of the forward (k_{flip}) and reverse (k_{unflip}) rate constants for flipping (eq 8). Similar results were obtained with the 19TεC substrate, but the fluorescence change was much smaller (Figure S7 of the Supporting Information). Although we cannot tell from these data whether there is a detectable signal for binding of AlkA prior to nucleotide flipping, the rapid concentration-independent nucleotide flipping establishes that DNA binding is very fast. We can estimate a lower limit for the association rate constant (k_{on}) of 3×10^9 M^{-1} s^{-1}, because binding must be at least 10-fold faster than the concentration-independent change in fluorescence (Figure 5D and eq 9). There is no evidence of the formation of a nonspecific AlkA·DNA complex, suggesting that if this forms it quickly converts to the specific complex. However, multiple AlkA proteins can bind under conditions of excess AlkA, and this could obscure a slower searching process. Therefore, it can be informative to test conditions of excess DNA (see below).

Nucleotide Unflipping and Dissociation from DNA. To test whether AlkA is committed to catalysis once it binds εA-DNA, we performed a single-turnover pulse-chase assay. AlkA was incubated with 19TεC substrate for 20 s before the addition of excess tight binding pyrrolidine (py-DNA) chase. AlkA will thus be bound to the flipped out εA as formation of the specific complex occurs on the millisecond time scale (Figure 5B), but excision occurs on the minute time scale (Figure 2). No εA excision was detected after the addition of chase (Figure 6A), indicating that the specific AlkA complex is not committed to base excision and rapidly dissociates. Assuming that 5% product could have been readily observed, the value of the observed rate constant for dissociation of the εA-DNA·AlkA complex ($k_{off,obs}$) must be at least 20-fold faster than the rate constant for N-glycosidic bond hydrolysis (eq 11). A lower limit of 0.09 s^{-1} can therefore be assigned for $k_{off,obs}$.

Given that AlkA is not committed to catalysis, and all of the substrate dissociates in the presence of chase, we turned to double-mixing stopped-flow experiments to directly measure the dissociation of substrate. These experiments were

DOI: 10.1021/bi501356x
Biochemistry 2015, 54, 898−908

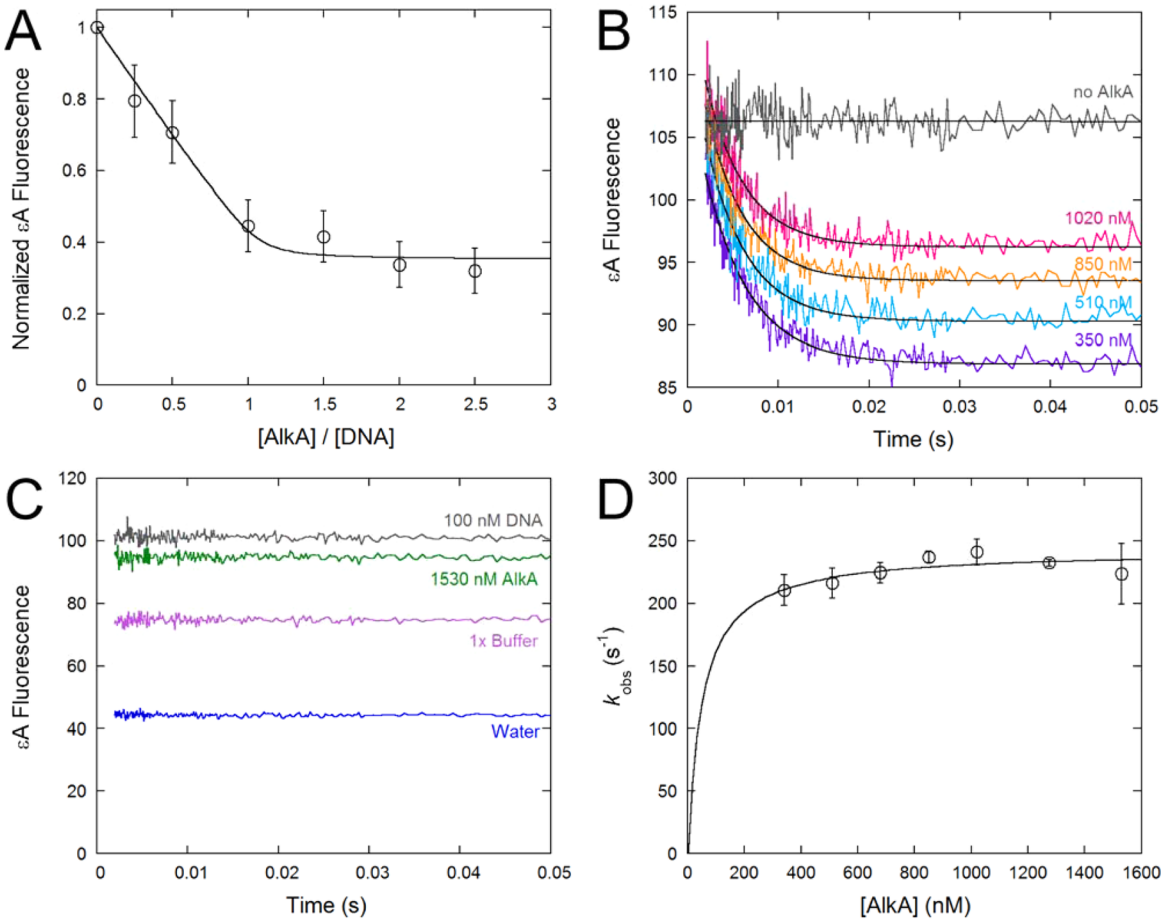

Figure 5. Quenching of εA fluorescence by AlkA indicates rapid nucleotide flipping. (A) Steady state quenching of εA-DNA fluorescence was measured using 400 nM 19AεA DNA and increasing concentrations of AlkA. The normalized fluorescence was fit by a 1:1 binding model (eq 7). The average ± SD is shown (n = 4). (B) Representative time-dependent changes in εA-DNA fluorescence as observed by single-mixing stopped-flow experiments with 19AεA substrate (100 nM) and varying excesses of AlkA. The fluorescence is reported in arbitrary units, and each trace is the average of three shots. Data were fit by a single exponential. (C) Controls to evaluate the signal-to-noise ratio. The fluorescence signal of 100 nM 19AεA substrate was set to 100, and the signals from water, buffer, or the highest AlkA concentration alone are shown. (D) The k_{obs} values from single exponentials were plotted vs AlkA concentration and fit with a hyperbolic function. This fit does not yield information regarding the $K_{1/2}$ for AlkA binding, because there is not sufficient signal to test lower concentrations of AlkA. The maximal value of 242 ± 11 s^{-1} is independent of AlkA concentration above 850 nM AlkA. The average ± SD is shown ($n \geq 2$).

performed with ratios of reagents similar to those used in the pulse-chase assay. AlkA and 19AεA were mixed and aged for 5 s to allow for the formation of the specific complex, which was subsequently chased with py-DNA competitor. A single-exponential increase in εA fluorescence was observed as the εA-DNA dissociates from AlkA (Figure 6B; $k_{off,obs}$ = 52 ± 2 s^{-1}). The length of the age time (1 or 5 s) and the concentration of chase (3 or 10 μM) did not affect the value of $k_{off,obs}$ that was obtained (Figure S8 of the Supporting Information).

We hypothesized that the slow step in dissociation of εA-DNA would correspond to unflipping of the εA lesion, followed by rapid dissociation from DNA. However, if dissociation from undamaged DNA was on the same time scale as flipping, then this could complicate the interpretation. Therefore, we also performed a stopped-flow experiment to assay the dissociation of AlkA from undamaged DNA (Figure 7). In this experiment, the nonspecific complex is first formed between AlkA and undamaged DNA and then mixed with a saturating amount of 19AεA substrate. The signal of binding of εA-DNA to AlkA is monitored, but the observed rate constant is dependent on both AlkA dissociation and association. The contribution from the dissociation step can be determined by comparing this rate constant to the rate constant obtained for the binding of free AlkA to εA-DNA under the same conditions. In the stopped-flow experiment with free AlkA and excess DNA, the εA fluorescence is quenched in a single phase with an observed rate constant of 233 ± 11 s^{-1} (Figure 7, purple trace). This value is almost identical to the value that was observed with excess AlkA protein [$k_{flip,obs}$ = 242 ± 11 s^{-1} (Figure 4)]. This observation suggests that the searching steps (k_{find}) performed by a single AlkA molecule are very rapid. When the nonspecific AlkA·DNA complex was mixed with excess εA-DNA, the single phase was slowed slightly with a k_{obs} value of 186 ± 7 s^{-1}. The modest reduction in rate indicates that AlkA dissociates very quickly from undamaged DNA with a rate constant of 920 s^{-1} (eq 10). This confirms that the unflipping step is almost fully rate-limiting for the dissociation of AlkA from the specific complex with εA-DNA.

Calculation of the Kinetic and Thermodynamic Framework. Many of the experiments that were performed do not directly yield microscopic rate constants, because of the

DOI: 10.1021/bi501356x
Biochemistry 2015, 54, 898−908

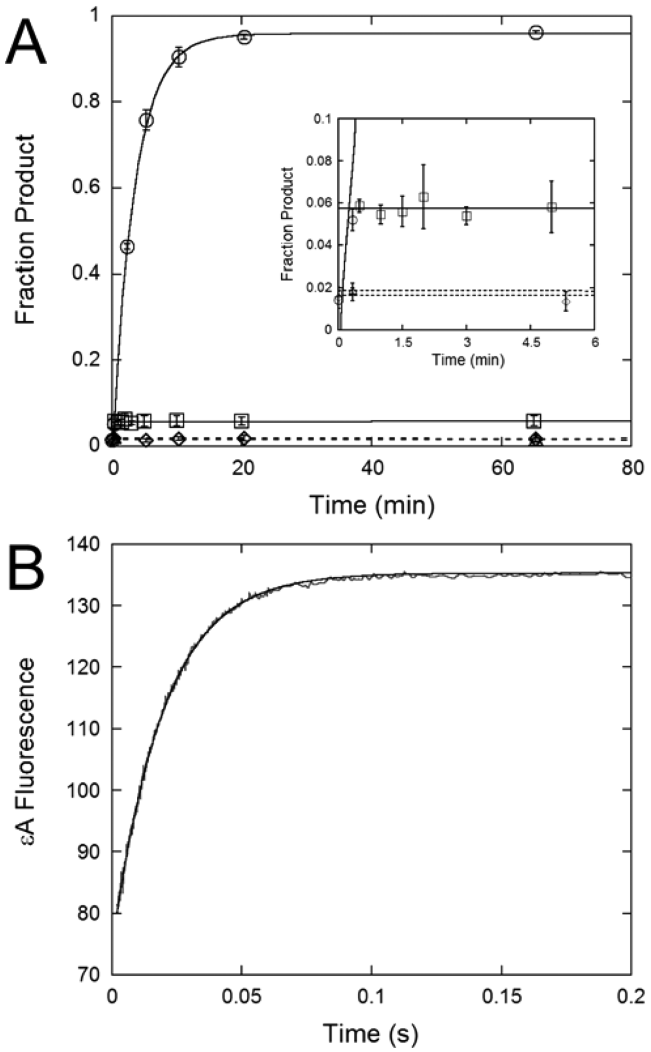

Figure 6. AlkA unflips εA and dissociates rapidly. (A) Time course for single-turnover pulse-chase assay. 19TεC substrate (100 nM) was mixed with 850 nM AlkA, aged for 20 s, and mixed with 10 μM 25TpyC chase. The reaction without chase (○) was fit by a single exponential matching that in Figure 1A. The reaction with chase (□) was fit by a straight line, as zero percent of the reaction progressed after the 20 s age time. No enzyme (△) and premixed εA and chase controls (◇) show no reaction occurring. The inset shows the low fraction product data showing that no εA excision occurred in the presence of chase. The average ± SD is shown (n = 3). (B) Representative εA-DNA fluorescence from a double-mixing stopped-flow assay in which AlkA (425 nM) and 19AεA DNA (200 nM) were mixed, aged for 5 s, and mixed with 25TpyC chase (3 μM). Data were fit by a single exponential with a $k_{off,obs}$ value of 51 s^{-1}. Fluorescence is reported in arbitrary units and is the average of three shots. Replicates give an average $k_{off,obs}$ value of 52 ± 2 s^{-1} (Figure S8 of the Supporting Information).

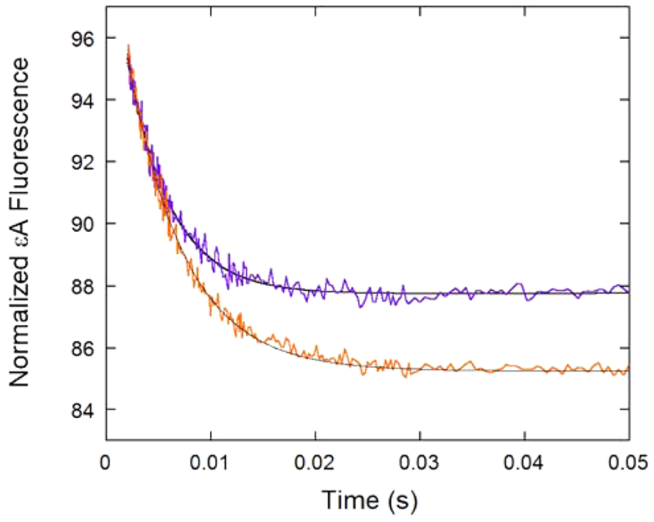

Figure 7. Association of AlkA under conditions of excess DNA and measurement of dissociation from nonspecific DNA. Representative εA-DNA fluorescence when AlkA (1 μM) was mixed with excess 19AεA substrate (5 μM) in the stopped flow (purple). The single phase was fit by a single exponential and gave a k_{obs} value of 233 ± 11 s^{-1}. The nonspecific AlkA·DNA complex was formed by preincubating AlkA with 25TAC DNA (500 nM). This complex was mixed with 19AεA DNA (orange), showing a single exponential with a k_{obs} value of 186 ± 7 s^{-1}. Fluorescence traces are the average of triplicate reactions from a single day, and the arbitrary fluorescence was normalized by dividing by the expected value at the time of mixing and multiplying by 100. This experiment was repeated, and the reported rate constants reflect the average ± SD (n = 3).

reversibility or multiple steps that are partially rate-limiting. However, these independent experiments could be combined to determine the individual kinetic parameters (Figure 8). These calculations are briefly described below, and the equations and additional details are provided in Materials and Methods.

The association and dissociation steps for AlkA are very fast and the most poorly defined parameters that we have measured. The rate of dissociation of undamaged DNA was calculated to be 920 s^{-1} (Figure 7; see the text above). Using this value and the K_d value for nonspecific sites (1.2 μM) that was determined by competition (Figure 4), an association rate constant of 8 × 10^8 M^{-1} s^{-1} can be calculated ($k_{on} = k_{off}/K_d$). This value is consistent with the 3 × 10^9 M^{-1} s^{-1} limit estimated from the rapid binding of AlkA with εA-DNA (Figure 5D). Assuming that AlkA binds to its εA substrate, abasic DNA, and undamaged DNA at the same rate, we can use the K_d value of the abasic product [1.2 nM (Figure 3)] to calculate a value of 1 s^{-1} for the product dissociation ($k_{off} = k_{on}K_d$). This calculated dissociation rate constant is much faster than the steady state k_{cat} value of 0.004 s^{-1}, consistent with the conclusion that N-glycosidic bond hydrolysis is rate-limiting for multiple- and single-turnover reactions. After AlkA binds to a nonspecific site, it must find the site of damage. These DNA searching steps (k_{find}) are all much faster than the rate of nucleotide flipping, because identical reaction rates are observed under conditions of excess DNA [where each protein needs to conduct its search independently (Figure 7)] and conditions of excess protein [where the searching time will be accelerated by having many proteins searching (Figure 5D)].

The rates and equilibrium constants for nucleotide flipping can be calculated from the forward and reverse binding reactions. The nucleotide unflipping step is the rate-limiting step in the dissociation reaction, as the $k_{off,obs}$ value of 52 s^{-1} (Figure 6B) is much slower than the k_{off} value of 920 s^{-1}. Combining these results with the observed rate constant for flipping in the forward direction [$k_{flip,obs}$ = 242 s^{-1} (Figure 5D)] yields a value of 62 s^{-1} for k_{unflip} (eq 13). By subtracting the k_{unflip} value from the observed flipping rate constant, we find the forward rate constant for flipping (k_{flip}) to be 180 s^{-1} (eq 8). The equilibrium constant for flipping of 2.9 is defined as the ratio of the nucleotide flipping and unflipping rate constants

DOI: 10.1021/bi501356x
Biochemistry 2015, 54, 898−908

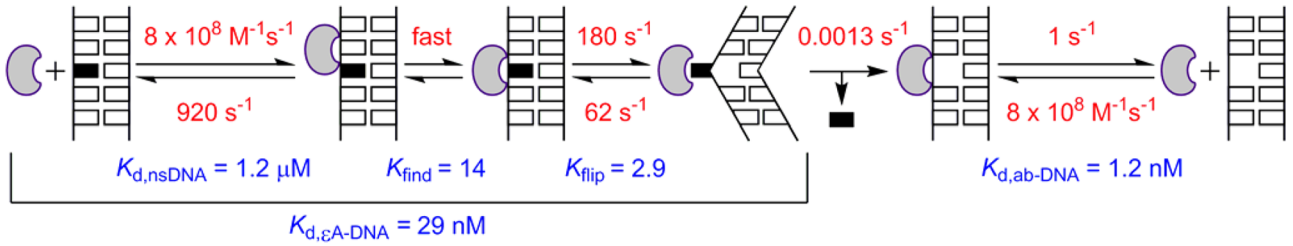

Figure 8. Minimal kinetic mechanism for AlkA-catalyzed excision of εA. Rate constants are colored red and equilibrium constants blue. The internal equilibria, K_{find} for locating the site of damage and K_{flip} for flipping out the damaged nucleotide, are expressed in the forward direction. We assume that AlkA has a mechanism for binding abasic DNA similar to that for binding damaged nucleotides, with nonspecific binding, fast searching, and flipping of the abasic nucleotide. These steps are omitted for the sake of clarity. The affinity for the abasic site is ∼1000-fold tighter than for a nonspecific site, which includes both the equilibrium for flipping and the equilibrium for finding the site. The values describe the reaction at 25 °C (see the Supporting Information).

(K_{flip} = k_{flip}/k_{unflip}). This indicates that the extrahelical recognition complex is only slightly favorable for AlkA.

The stopped-flow fluorescence studies demonstrate that DNA binding, searching, and nucleotide flipping are all much faster than base excision. Therefore, the single-turnover rate constant is approximately equal to the rate constant for N-glycosidic bond cleavage (k_{chem}), and the $K_{1/2}$ is equal to the K_d for εA-DNA (Figure 3B). For this multistep binding mechanism, the overall dissociation constant for the AlkA·εA-DNA complex is the product of the individual equilibria along the reaction coordinate ($K_{d,\varepsilon A\text{-}DNA}$ = $K_{d,nsDNA}$ × 1/K_{find} × 1/K_{flip}). Thus, we were able to obtain an estimate for the equilibrium between nonspecific sites and the lesion site [K_{find} = 14 (Figure 8)]. This indicates that AlkA is able to bind significantly more tightly to an εA·T site than to a nonspecific site even prior to the nucleotide flipping step.

DISCUSSION

We report the minimal kinetic and thermodynamic framework for the AlkA-catalyzed excision of εA, including measurements for DNA binding and nucleotide flipping. This framework reveals some clear differences in substrate recognition by AlkA and AAG, two glycosylases that independently evolved to have similar functions in protecting the genome against alkylative DNA damage.

Minimal AlkA Mechanism. Previous studies of AlkA have assumed that the slow glycosylase activity reflects rate-limiting N-glycosidic bond hydrolysis; however, it was not possible to rule out the alternative model that binding or nucleotide flipping is rate-limiting.[22,25] By directly measuring the rates for binding and nucleotide flipping with εA-DNA, we confirmed that hydrolysis is the rate-limiting step for AlkA. All of the other steps in the AlkA mechanism are much faster than this step, which ensures that εA-DNA is sampled and rejected many times prior to being excised (Figure 8). This mechanism is consistent with a generalist strategy of removing many different damaged bases with a wide range of shapes and chemical properties.

The overall affinity for εA-DNA is 40-fold tighter than for a nonspecific site, demonstrating specific recognition of this damaged base. However, given the vast excess of undamaged sites, this specificity is unlikely to allow for efficient targeting of εA lesions *in vivo*. This is consistent with the results from deletion experiments suggesting that direct repair is responsible for the majority of εA repair in *E. coli*.[32] Nevertheless, the origin of this 40-fold specificity is interesting and potentially informative for understanding how AlkA recognizes other lesions. We determined a K_{flip} value of 3, which indicates that the flipping of εA into the active site of AlkA provides only 3-fold stabilization relative to a bound state in which εA is not flipped out. By independently measuring the affinity of undamaged DNA and the overall equilibrium constant for εA-DNA binding, we can calculate a theoretical value for binding to the damaged site (K_{find} = 14). We do not know the nature of this early recognition complex, but it may take advantage of DNA intercalation and/or DNA bending to achieve tighter binding.

Our kinetic experiments reveal that AlkA searches DNA very rapidly. Many other DNA glycosylases use facilitated diffusion to search DNA for sites of damage, and in most cases, strong electrostatic interactions are an important feature.[35−38] However, the AlkA DNA binding interface is not positively charged, and few electrostatic DNA contacts are observed in crystal structures of AlkA·DNA complexes.[19] This raises the possibility that the searching mechanism of AlkA may be quite different from those employed by other glycosylases.

Biochemical assays suggest that a major role of AlkA is to remove positively charged alkylated bases bearing a destabilized N-glycosidic bond. The substrates have sites of alkylation that include N3 and N7 of purines and O2 of pyrimidines.[9,39] It appears that AlkA has adopted a strategy of providing similar rate enhancement for excision of these damaged bases and undamaged nucleotides that have more stable N-glycosidic bonds.[13,22] For this mechanism to operate, it is important that AlkA rapidly search DNA and sample nucleotides in its active site. The kinetic parameters that we have described for the excision of εA support this model. Although this mechanism provides very broad protection, it does have a cost associated with it, in the removal of undamaged bases.[13] Indeed, overexpression of AlkA causes increased frequency of mutations attributed to larger numbers of abasic sites.[13,40] *E. coli* minimizes this cost by controlling the expression of AlkA, inducing its expression under conditions of chronic exposure to DNA alkylation damage as part of the ada transcriptional response.[15]

We found that AlkA binds more than 20-fold more tightly to the abasic product than to the εA lesion. This suggests that AlkA flips out the abasic site to allow for more favorable contacts with the DNA, and it is likely that the crystal structure of AlkA bound to the abasic site analogue 1-aza-2′-deoxyribose is a reasonable model for this complex. In this structure, the DNA is sharply bent, the sugar is flipped out, and a conserved leucine (L125) intercalates into the DNA duplex.[19] Although it has been proposed that DNA glycosylases protect reactive

DOI: 10.1021/bi501356x
Biochemistry 2015, 54, 898−908

abasic sites from undesirable reactions, it has been observed that AlkA catalyzes promiscuous reactions of abasic sites with alcohols to generate O-glycosidic DNA adducts.[34] Despite this tight binding, the observed dissociation is very fast and unlikely to limit the rate of AlkA catalysis on known substrates.

Comparisons between AlkA and AAG. AlkA and AAG independently evolved to remove an extensive set of alkylated and oxidatively damaged bases, but they operate under different physiological niches. Hoth glycosylases show *in vitro* activity on the cyclic adduct εA,[11] allowing us to directly compare their mechanisms.

Given their independent evolution, it is striking that there are some structural parallels between AlkA and AAG. Both enzymes have conserved carboxylate groups to position a water molecule and directly hydrolyze the N-glycosidic bond, and both use DNA intercalation to stabilize a flipped out lesion.[6] However, the three-dimensional structure and identity of the residues that contact the DNA are completely different for the two enzymes. Remarkably, the rates of N-glycosidic bond cleavage are almost identical when measured under similar reaction conditions (Table S1 of the Supporting Information).[26] In contrast, the affinities for εA-DNA are dramatically different. AlkA binds εA-DNA relatively weakly with a K_d value of 29 nM compared to a value of 20 pM for AAG.[23] The difference in binding makes AAG 1000-fold more efficient than AlkA at εA removal (Table S1 of the Supporting Information). Crystal structures of AAG bound to εA-DNA reveal favorable contacts with the εA nucleobase, including a hydrogen bond between a backbone amide and N6 of εA.[18] This suggests that AAG has evolved to recognize εA as an important physiological substrate, whereas AlkA exhibits fortuitous activity. Whereas DNA binding is similarly fast for both enzymes, the rate constants for flipping and unflipping are very different. Flipping is 50-fold slower and unflipping 40000-fold slower for AAG than for AlkA. This reflects an 800-fold difference in the equilibrium constant for nucleotide flipping (Table S1 of the Supporting Information). Furthermore, the slow unflipping by AAG causes a strong commitment to catalysis such that most DNA binding events are productive. As discussed above, AlkA exhibits rapid reversible εA-DNA binding without any commitment to catalysis, allowing it to quickly sample a structurally diverse set of damaged bases.

Recently, a mutant of AAG in which the intercalating residue (Y162) was mutated to alanine was described.[26] This residue is critical for stabilizing the extrahelical εA complex. The Y162A AAG mutant is no longer committed to excision of εA, and its behavior is remarkably similar to that of wild-type (WT) AlkA. The rate constant for nucleotide flipping by Y162A AAG is virtually identical to that of AlkA [170 s^{-1} compared to 180 s^{-1} (Table S1 of the Supporting Information)]. The Y162A AAG mutant also exhibits a K_{flip} value of 17, which is much closer to that of AlkA than that of WT AAG. Thus, it appears that many of the kinetic differences between AlkA and AAG can be attributed to the intercalating tyrosine that is found in AAG. In AAG, this residue allows for much more stable binding of the extrahelical lesion but also slows the nucleotide flipping step. Although it is clearly an oversimplification to attribute the differences between enzymes to a single interaction, it is intriguing to note that kinetic studies of other DNA glycosylases show a similar trend. Uracil DNA glycosylase, like AlkA, uses an intercalating leucine and exhibits very rapid nucleotide flipping (k_{flip} = 1200 s^{-1}).[26,27] Formamidopyrimidine DNA glycosylase employs an intercalating phenylalanine that is more similar to the tyrosine that AAG uses, and this enzyme exhibits slower nucleotide flipping (k_{flip} = 1−12 s^{-1}).[41−43] Additional mutational studies are needed to understand the mechanistic differences between the different families of DNA repair enzymes.

Conclusions. By directly measuring DNA binding and nucleotide flipping, we have gained new insights into how AlkA recognizes DNA damage. We expect that the fast flipping and rapid searching that we have observed for an εA-DNA substrate will extend to other substrates of AlkA, and the N-glycosidic bond cleavage step is likely to be rate-limiting for most substrates. By rapidly and reversibly sampling sites, AlkA is able to maintain a remarkably promiscuous active site pocket that accommodates damaged bases of very different sizes. This strategy is ideally suited to alkyl adducts that have destabilized N-glycosidic bonds, because little catalytic power is needed to perform the reaction on a biologically relevant time scale.

■ ASSOCIATED CONTENT

Supporting Information

Additional experiments with varying substrates and conditions and a table of comparisons to AAG. This material is available free of charge via the Internet at http://pubs.acs.org.

■ AUTHOR INFORMATION

Corresponding Author

*E-mail:pjobrien@umich.edu. Phone: (734) 647-5821.

Funding

This work was supported by National Institutes of Health Grants T32 GM008597 to E.L.T. and GM108022 to P.J.O.

Notes

The authors declare no competing financial interest.

■ ACKNOWLEDGMENTS

We thank everyone in the O'Brien lab for helpful advice and comments.

■ ABBREVIATIONS

AlkA, 3-methyladenine DNA glycosylase II; AAG, alkyladenine DNA glycosylase, also known as MPG, methyl-purine DNA glycosylase; 3meA, N^3-methyladenine; 7meG, N^7-methylguanine; εA, 1,N^6-ethenoadenine; ab, abasic site; BER, base excision repair; FAM, 6-carboxyfluorescein; HEX, 6-hexachlorofluorescein; hx, hypoxanthine; MMS, methylmethanesulfonate; ns, nonspecific site; py, pyrrolidine; SD, standard deviation.

■ REFERENCES

(1) Lindahl, T. (1993) Instability and decay of the primary structure of DNA. *Nature 362*, 709−715.

(2) Marnett, L. J., Riggins, J. N., and West, J. D. (2003) Endogenous generation of reactive oxidants and electrophiles and their reactions with DNA and protein. *J. Clin. Invest. 111*, 583−593.

(3) Beranek, D. T. (1990) Distribution of methyl and ethyl adducts following alkylation with monofunctional alkylating agents. *Mutat. Res. 231*, 11−30.

(4) Sedgwick, B. (2004) Repairing DNA-methylation damage. *Nat. Rev. Mol. Cell Biol. 5*, 148−157.

(5) O'Brien, P. J. (2006) Catalytic promiscuity and the divergent evolution of DNA repair enzymes. *Chem. Rev. 106*, 720−752.

(6) Hollis, T., Lau, A., and Ellenberger, T. (2001) Crystallizing thoughts about DNA base excision repair. *Prog. Nucleic Acid Res. Mol. Biol. 68*, 305−314.

DOI: 10.1021/bi501356x
Biochemistry 2015, 54, 898−908

(7) Denver, D. R., Swenson, S. L., and Lynch, M. (2003) An evolutionary analysis of the helix-hairpin-helix superfamily of DNA repair glycosylases. *Mol. Biol. Evol. 20*, 1603−1611.
(8) Eisen, J. A., and Hanawalt, P. C. (1999) A phylogenomic study of DNA repair genes, proteins, and processes. *Mutat. Res. 435*, 171−213.
(9) Thomas, L., Yang, C. H., and Goldthwait, D. A. (1982) Two DNA glycosylases in *Escherichia coli* which release primarily 3-methyladenine. *Biochemistry 21*, 1162−1169.
(10) Engelward, B. P., Weeda, G., Wyatt, M. D., Broekhof, J. L., de Wit, J., Donker, I., Allan, J. M., Gold, B., Hoeijmakers, J. H., and Samson, L. D. (1997) Base excision repair deficient mice lacking the Aag alkyladenine DNA glycosylase. *Proc. Natl. Acad. Sci. U.S.A. 94*, 13087−13092.
(11) Saparbaev, M., Kleibl, K., and Laval, J. (1995) *Escherichia coli*, *Saccharomyces cerevisiae*, rat and human 3-methyladenine DNA glycosylases repair 1,N6-ethenoadenine when present in DNA. *Nucleic Acids Res. 23*, 3750−3755.
(12) Saparbaev, M., and Laval, J. (1994) Excision of hypoxanthine from DNA containing dIMP residues by the *Escherichia coli*, yeast, rat, and human alkylpurine DNA glycosylases. *Proc. Natl. Acad. Sci. U.S.A. 91*, 5873−5877.
(13) Berdal, K. G., Johansen, R. F., and Seeberg, E. (1998) Release of normal bases from intact DNA by a native DNA repair enzyme. *EMBO J. 17*, 363−367.
(14) O'Brien, P. J., and Ellenberger, T. (2004) Dissecting the broad substrate specificity of human 3-methyladenine-DNA glycosylase. *J. Biol. Chem. 279*, 9750−9757.
(15) Evensen, G., and Seeberg, E. (1982) Adaptation to alkylation resistance involves the induction of a DNA glycosylase. *Nature 296*, 773−775.
(16) Sedgwick, B., and Lindahl, T. (2002) Recent progress on the Ada response for inducible repair of DNA alkylation damage. *Oncogene 21*, 8886−8894.
(17) Samson, L., and Cairns, J. (1977) A new pathway for DNA repair in *Escherichia coli*. *Nature 267*, 281−283.
(18) Lau, A. Y., Wyatt, M. D., Glassner, B. J., Samson, L. D., and Ellenberger, T. (2000) Molecular basis for discriminating between normal and damaged bases by the human alkyladenine glycosylase, AAG. *Proc. Natl. Acad. Sci. U.S.A. 97*, 13573−13578.
(19) Hollis, T., Ichikawa, Y., and Ellenberger, T. (2000) DNA bending and a flip-out mechanism for base excision by the helix-hairpin-helix DNA glycosylase, *Escherichia coli* AlkA. *EMBO J. 19*, 758−766.
(20) O'Brien, P. J., and Ellenberger, T. (2003) Human alkyladenine DNA glycosylase uses acid-base catalysis for selective excision of damaged purines. *Biochemistry 42*, 12418−12429.
(21) Labahn, J., Scharer, O. D., Long, A., Ezaz-Nikpay, K., Verdine, G. L., and Ellenberger, T. E. (1996) Structural basis for the excision repair of alkylation-damaged DNA. *Cell 86*, 321−329.
(22) O'Brien, P. J., and Ellenberger, T. (2004) The *Escherichia coli* 3-methyladenine DNA glycosylase AlkA has a remarkably versatile active site. *J. Biol. Chem. 279*, 26876−26884.
(23) Wolfe, A. E., and O'Brien, P. J. (2009) Kinetic mechanism for the flipping and excision of 1,N(6)-ethenoadenine by human alkyladenine DNA glycosylase. *Biochemistry 48*, 11357−11369.
(24) Baldwin, M. R., and O'Brien, P. J. (2009) Human AP endonuclease 1 stimulates multiple-turnover base excision by alkyladenine DNA glycosylase. *Biochemistry 48*, 6022−6033.
(25) Zhao, B., and O'Brien, P. J. (2011) Kinetic mechanism for the excision of hypoxanthine by *Escherichia coli* AlkA and evidence for binding to DNA ends. *Biochemistry 50*, 4350−4359.
(26) Hendershot, J. M., and O'Brien, P. J. (2014) Critical role of DNA intercalation in enzyme-catalyzed nucleotide flipping. *Nucleic Acids Res. 42*, 12681−12690.
(27) Pandya, G. A., and Moriya, M. (1996) 1,N6-Ethenodeoxyadenosine, a DNA adduct highly mutagenic in mammalian cells. *Biochemistry 35*, 11487−11492.
(28) Nair, J., Barbin, A., Velic, I., and Bartsch, H. (1999) Etheno DNA-base adducts from endogenous reactive species. *Mutat. Res. 424*, 59−69.
(29) Gros, L., Ishchenko, A. A., and Saparbaev, M. (2003) Enzymology of repair of etheno-adducts. *Mutat. Res. 531*, 219−229.
(30) Calvo, J. A., Meira, L. B., Lee, C. Y., Moroski-Erkul, C. A., Abolhassani, N., Taghizadeh, K., Eichinger, L. W., Muthupalani, S., Nordstrand, L. M., Klungland, A., and Samson, L. D. (2012) DNA repair is indispensable for survival after acute inflammation. *J. Clin. Invest. 122*, 2680−2689.
(31) Delaney, J. C., Smeester, L., Wong, C., Frick, L. E., Taghizadeh, K., Wishnok, J. S., Drennan, C. L., Samson, L. D., and Essigmann, J. M. (2005) AlkB reverses etheno DNA lesions caused by lipid oxidation in vitro and in vivo. *Nat. Struct. Mol. Biol. 12*, 855−860.
(32) Maciejewska, A. M., Sokolowska, B., Nowicki, A., and Kusmierek, J. T. (2011) The role of AlkB protein in repair of 1,N(6)-ethenoadenine in *Escherichia coli* cells. *Mutagenesis 26*, 401−406.
(33) Scharer, O. D., Nash, H. M., Jiricny, J., Laval, J., and Verdine, G. L. (1998) Specific binding of a designed pyrrolidine abasic site analog to multiple DNA glycosylases. *J. Biol. Chem. 273*, 8592−8597.
(34) Admiraal, S. J., and O'Brien, P. J. (2013) DNA-N-glycosylases process novel O-glycosidic sites in DNA. *Biochemistry 52*, 4066−4074.
(35) Ganesan, A. K., Seawell, P. C., Lewis, R. J., and Hanawalt, P. C. (1986) Processivity of T4 endonuclease V is sensitive to NaCl concentration. *Biochemistry 25*, 5751−5755.
(36) Hedglin, M., Zhang, Y., and O'Brien, P. J. (2013) Isolating contributions from intersegmental transfer to DNA searching by alkyladenine DNA glycosylase. *J. Biol. Chem. 288*, 24550−24559.
(37) Schonhoft, J. D., Kosowicz, J. G., and Stivers, J. T. (2013) DNA translocation by human uracil DNA glycosylase: Role of DNA phosphate charge. *Biochemistry 52*, 2526−2535.
(38) Francis, A. W., and David, S. S. (2003) *Escherichia coli* MutY and Fpg utilize a processive mechanism for target location. *Biochemistry 42*, 801−810.
(39) Bjelland, S., Birkeland, N. K., Benneche, T., Volden, G., and Seeberg, E. (1994) DNA glycosylase activities for thymine residues oxidized in the methyl group are functions of the AlkA enzyme in *Escherichia coli*. *J. Biol. Chem. 269*, 30489−30495.
(40) Frosina, G. (2000) Overexpression of enzymes that repair endogenous damage to DNA. *Eur. J. Biochem. 267*, 2135−2149.
(41) Fedorova, O. S., Nevinsky, G. A., Koval, V. V., Ishchenko, A. A., Vasilenko, N. L., and Douglas, K. T. (2002) Stopped-flow kinetic studies of the interaction between *Escherichia coli* Fpg protein and DNA substrates. *Biochemistry 41*, 1520−1528.
(42) Koval, V. V., Kuznetsov, N. A., Zharkov, D. O., Ishchenko, A. A., Douglas, K. T., Nevinsky, G. A., and Fedorova, O. S. (2004) Pre-steady-state kinetics shows differences in processing of various DNA lesions by *Escherichia coli* formamidopyrimidine-DNA glycosylase. *Nucleic Acids Res. 32*, 926−935.
(43) Kuznetsov, N. A., Koval, V. V., Zharkov, D. O., Vorobjev, Y. N., Nevinsky, G. A., Douglas, K. T., and Fedorova, O. S. (2007) Pre-steady-state kinetic study of substrate specificity of *Escherichia coli* formamidopyrimidine−DNA glycosylase. *Biochemistry 46*, 424−435.

DOI: 10.1021/bi501356x
Biochemistry 2015, 54, 898−908